ISSN (Print) 1226-1750
ISSN (Online) 2233-6656
Journal of Magnetics 25(4), 699-703 (2020) https://doi.org/10.4283/JMAG.2020.25.4.699

Spring Displacement Sensor Composed of LC Resonance Circuit

Kyung-Won Kim and Kwang-Ho Shin*

Dept. of Information & Communication Engineering of Kyungsung University, 110-1 Daeyeon-dong Namgu, Busan 48434, Republic of Korea

(Received 15 July 2018, Received in final form 20 December 2020, Accepted 21 December 2020)

This paper was prepared to assert that coil springs could be useful as displacement sensors as well as mechanical parts. We have investigated the displacement dependence on the inductance of a coil spring and resonance frequency of a simple LC circuit in which a coil spring took a part as an inductor. The changing ratio of inductance to displacement was 6.6 %/mm. Inductance and/or inductance change of a coil spring was explained with FEM simulation. The changing ratio of the output voltage, which was obtained with the LC circuit, to displacement was estimated to be 6.23 %/mm.

Keywords : Coil spring, displacement sensor, inductance, resonance frequency

1. Introduction

Coil springs have been used for a long time as mechanical parts in order to maintain proper elasticity and damping of various mechanical systems [1]. Well-designed coil springs are characterized by excellent mechanical properties including elasticity and damping properties and their capacity for mechanical energy storage [2]. On the other hand, inductance sensors as magnetic sensors have many applications and have been developed for a long time [3-14]. An inductance sensor has usually ferromagnetic core to form an inductor. When magnetic field is applied to the ferromagnetic core, the permeability is changed. Since the inductance is proportional to the permeability, the inductance is finally changed by an applied magnetic field. In the case of solenoid inductor, the inductance is also changed by its shape and size. It means that the inductance could be changed by elongation of the inductor. If made of insulated metal wire, the structure of the coil spring is identical with that of the basic inductor (air core solenoid inductor). Therefore, the mechanical spring could act as an inductor at the same time. Basically, the elongation of a coil spring is proportional to the displacement of the endpoint and/or the load attached to it. Because of the elongation also affects the inductance of the solenoid inductor of which shape is identical with a coil spring, the inductance changes by the displacement and/or the load. In other words, a coil spring is a variable inductance whose inductance changes due to displacement or load.

In this study, we have investigated experimentally the displacement dependences on inductance of the coil spring and of output voltage of an AC voltage divider circuit where the coil spring took a part as an inductor.

2. Experiment and Calculation

Figure 1 shows a photograph of the coil spring used in this study. The length and radius of the coil spring are 9.5 mm and 2.25 mm, respectively. This has solenoid shape

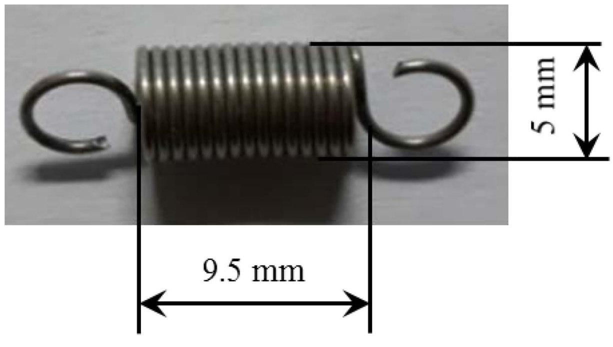

Fig. 1. Photograph of the coil spring.

*Corresponding author: Tel: +82-51-663-5152
Fax: +82-51-625-1402, e-mail: khshin@ks.ac.kr

This paper was presented at the IcAUMS2018, Jeju, Korea, June 3-7, 2018.

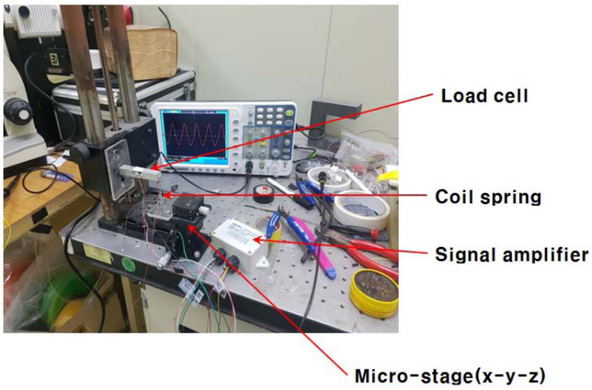

Fig. 2. (Color online) Photograph of experimental setup.

composed of 15.5 turns of a steel wire with the diameter of 0.5 mm. There are two hooks at both ends.

Figure 2 shows a photograph of experimental setup. One hook of the coil spring was attached to the end of a load cell (a kind of force sensor), while the other hook was attached to the surface of a microstage. The elongation of the coil spring was controlled by operating the microstage. When the length of coil spring is changed, the load force can be detected by the load cell. The inductance values dependent on the displacement and/or load force were checked by an LCR meter (Hioki 3522-50 LCR HiTester).

Exact calculation of inductance of coil spring is quite complicated due to several reasons; it can be done with space integration of magnetic flux [15]. Total inductance is the sum of the internal inductance, which should be calculated with certain conductivity and permeability dependent on frequency, and the external inductance [16]. Current distribution is affected by magnetic field generated by adjacent turns. This is known as the proximity effect. By the proximity effect, the effective area of each turn of wire is reduced, and hence the external inductance is also reduced [17].

Technically, the approximation formula, as shown in eq. 1, is often used to calculate the inductance of a solenoid [18, 19].

$$L = \frac{\mu_0 N^2 \pi a^2}{l} f\left(\frac{2a}{l}\right) \tag{1}$$

Where, a and l are the radius and the axial length of coil, respectively. N and μ_0 are the number of turns and vacuum permeability, respectively. The function f is known as the Nagaoka function [20]. In the case of $0 < 2a/l < 1$, the function f can be expressed as

$$f\left(\frac{2a}{l}\right) = f_1\left(\frac{4a^2}{l^2}\right) - \frac{4}{3\pi}\frac{2a}{l} \tag{2}$$

In eq. (1), the function f_1 is approximately 1 in the case of long solenoid. Therefore, eq. (1) can be denoted as

$$L = \frac{\mu_0 N^2 \pi a^2}{l}\left(1 - \frac{4}{3\pi}\frac{2a}{l}\right) \tag{3}$$

If all other parameters don't change, it is easy to understand that inductance would be inversely proportional to the length l.

A series of FEM simulations was also performed to calculate the inductance values dependent on elongation of the coil spring by using a commercial FEM package, COMSOL Multiphysics [21]. The governing equation for the FEM simulation was Ampere's law ($\nabla \times \vec{H} = \vec{J}$). The inductance of the coil spring was calculated by $\frac{2W_m}{I^2}$. Here, I and W_m are the current and the magnetic energy stored in the space around the coil spring.

3. Experimental and Simulation Results

Figure 3 shows FEM simulated magnetic field distributions around the coil spring in the case of coil pitch 0.6 mm (a) and 1.1 mm (b). As shown in Fig. 1, the magnetic field intensity decreases with elongation of the coil spring. Hence, the magnetic energy also decreases with elongation resulting in a reduced inductance. This tendency can be also predicted from eq. (3). The elongation dependence on inductance can be used to detect displacement of the object attached to the end of coil spring. Within elastic limit, the load force is directly proportional to the displacement of spring. It means that it is also possible to construct a force sensor with a coil spring and the inductance variation.

Figure 4 shows the displacement dependence on inductance of the coil spring. This graph represents a comparison between measured inductance and calculated ones. In this figure, three data are displayed together; measured data, FEM simulated data and calculated data by eq. (3). The measured values and the FEM simulated values are in very good agreement, but the calculated values by eq. (3) is slightly different from the others. As mentioned above, equation 3 is an approximate formula, and an integration of magnetic field is required to obtain an exact inductance value. However, because the three data show the same trend in Fig. 4, it is possible to explain the inductance variation analytically even with eq. (3). In this experiment, inductance of lead wire was 1.13 μH at 100 kHz with 10 mA. Considering the inductance of lead wire, the spring inductance changes from 235 nH to 375 nH with the displacement of 9 mm. The changing ratio of inductance to displacement $\Delta L/(\Delta l \cdot L_0)$ was

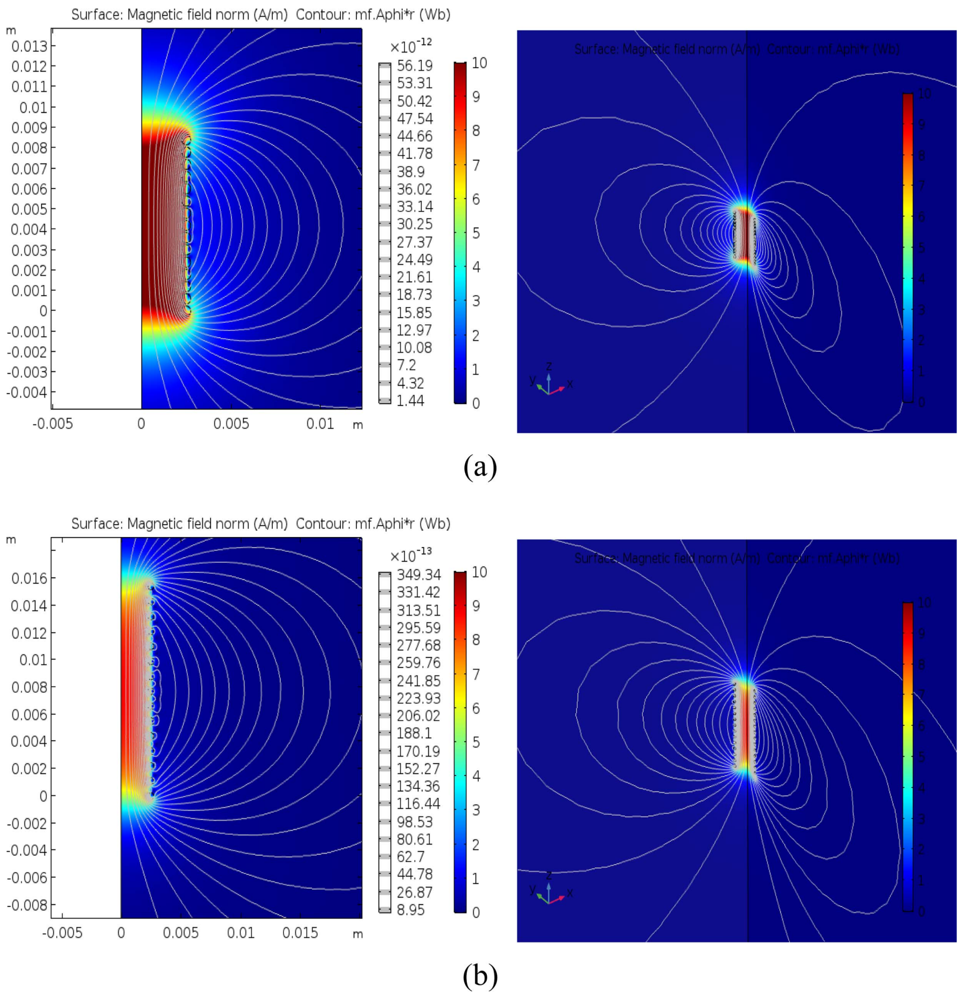

Fig. 3. (Color online) Magnetic field distribution around the coil spring: (a) Coil pitch 0.6 mm and (b) Coil pitch 1.1 mm.

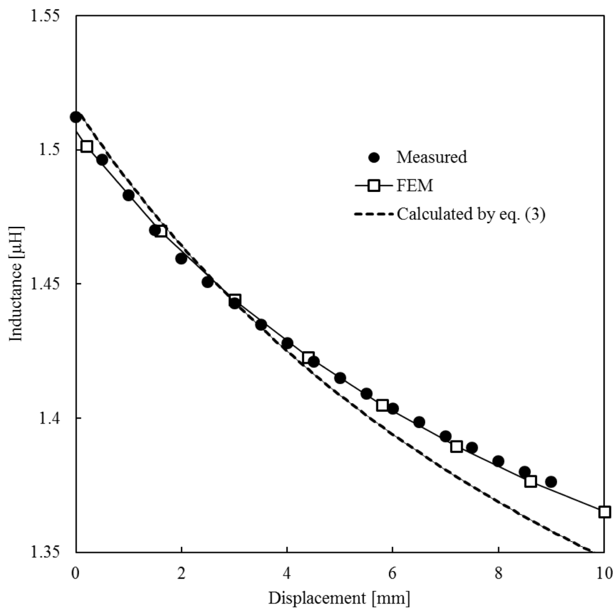

Fig. 4. Displacement dependence of inductance; measured, FEM simulated and calculated by eq. (3).

estimated to be 6.6 %/mm. This value will surely depend on the size and shape of the coil spring used. In the near future, we will quantitatively analyze the change rate of the inductance with respect to the shape and size of the spring.

From the results shown in Fig. 4, we were sure that the coil spring could be used as a displacement sensor. However, it is indispensable for use as a sensor to obtain a voltage output.

To make a coil spring to be a part of an electronic circuit, we have to know the circuit parameters, such as resistance as well as inductance. In this study, since it is hard to measure directly AC resistance at certain frequency, we tried to calculate the resistance of the coil spring. If we can assume the resistivity is constant in the measurement frequency region, AC resistance could be calculated by eq. (4)

$$R_{AC} = \rho \frac{l}{S_{eff}} \tag{4}$$

Where ρ is the resistivity of the conductor in Ω·m, and l and S_{eff} are, respectively, the length of the conductor in m and the effective cross sectional area used in m^2. The ρ was estimated to be 7.2 × 10^{-7} Ωm with reference to the literature. The l was estimated as 0.224 m. The S_{eff} could be defined by the skin effect which is for finding the nominal depth of current for a conductor. The skin depth could be calculated with eq. (5).

$$\delta = \sqrt{\frac{\rho}{\pi \mu_0 \mu_r f}} \tag{5}$$

Where f is the operation frequency in Hz. And μ_0 and μ_r are respectively vacuum permeability (4π × 10^{-7} H/m) and the relative permeability of the conductor which was assumed as 100. Now, we can calculate the S_{eff} with the skin depth δ as,

$$S_{eff} = \pi r^2 - \pi (r - \delta)^2 \tag{6}$$

From eq. (4)~(6), The AC resistance was estimated to be 3.15 Ω at the frequency of 1.5 MHz. Since we had the circuit parameters R and L, we could design a simple AC voltage divider circuit as shown in Fig. 5. *L_spring* and *R_spring* are the inductance and resistance of the coil spring. If we ignore *R_spring*, upside loop of *L_spring* and *C1* has the resonance frequency as

$$f_0 = \frac{1}{2\pi\sqrt{L\_spring \times C1}} \tag{7}$$

Since the *L_spring* is changed according to displacement, the f_0 also changes. For the circuit simulation which was done with a commercial tool Multisim [23], *R*2 and *L*2 were set to 3.15 W and 1.35 mH, respectively. *C1* and *C2* were set to 10 nF.

Figure 6 shows simulated output voltage (arbitrary value) in the frequency range of 1~2 MHz. From Fig. 6, it is easy to predict that we can large output voltage change dependent on inductance and displacement at the frequency of 1.2 MHz and 1.5 MHz. Surely, the optimum operation frequency can be designed by adjusting the parallel capacitors *C1* and *C2*. The larger capacitance the lower operation frequency.

Figure 7 shows the displacement dependence of output voltage measured with the circuit as shown Fig. 5 at the frequency of 1.5 MHz. There are two data sets with the same tendency, but slightly different values. We found out the output voltage could be changed by the condition of lead wire even if the frequency was not changed, because

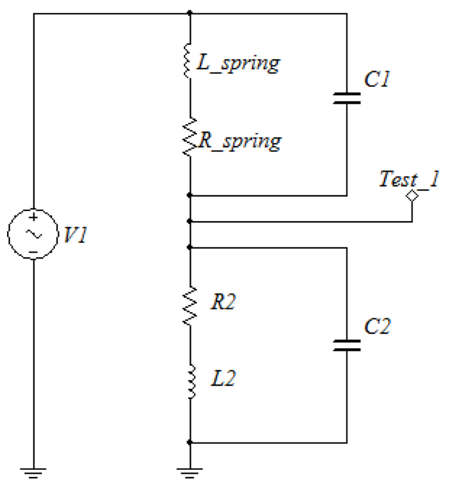

Fig. 5. AC voltage divider circuit to obtain the output voltage dependent on inductance.

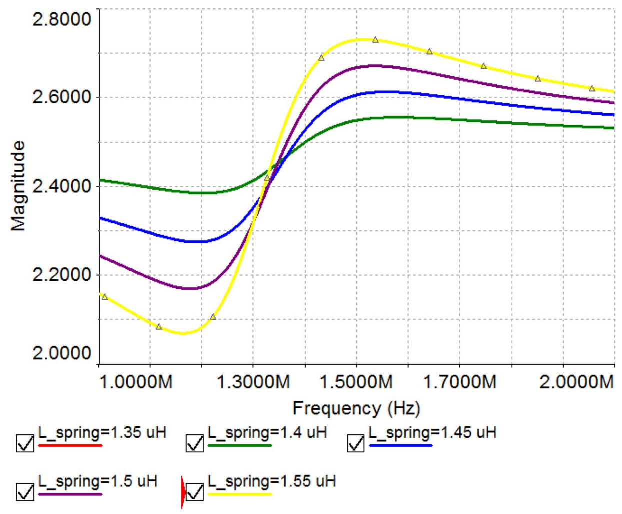

Fig. 6. (Color online) Simulated frequency dependence of output.

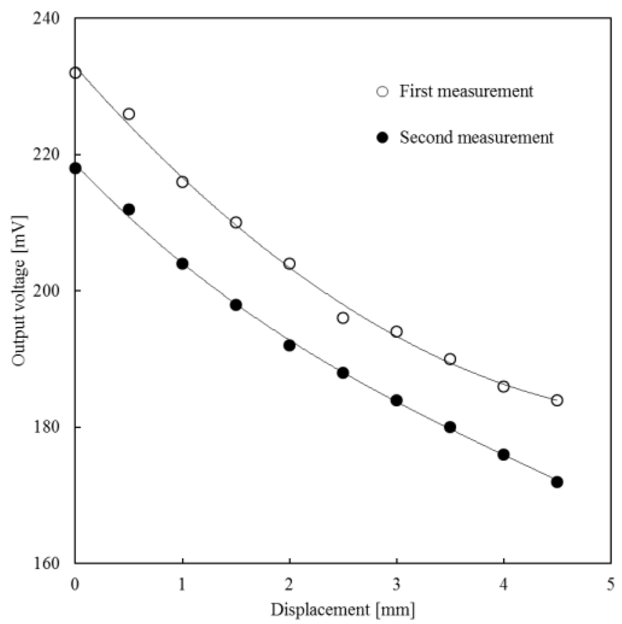

Fig. 7. Measured output voltage according to displacement.

the inductance of the lead wire could be changed by its bending and twisting state. However, we don't consider this is a major problem that makes the sensor application difficult. In practice, the lead wire will be fixed to the circuit so that the inductance does not change. In the first measurement in Fig. 7, the output voltage was changed from 218 mV to 170 mV with the displacement of 4.5 mm. The changing ratio of output voltage to displacement $\Delta V/(\Delta l \cdot V_0)$ was estimated to be 6.23 %/mm. And, the voltage change was 10.7 mV when displaced 1 mm. Generally, a voltage resolution of 1 μV is not so hard to be achieved using a suitable signal conditioning circuit such as a synchronous detection circuit. If we assume the voltage resolution is 1 μV, the displacement resolution would be under 100 nm. Here, we should mention the effect of the lead wire on the sensitivity. The inductance of the lead wire was ~1130 nH, even if changed slightly by its condition. This value was 4 times greater than the inductance of coil spring ~300 nH. Moreover the inductance of lead wire acts like a bias, so the sensitivity is lowered. To enhance the sensitivity, we will investigate how to minimize the inductance of lead wires or how to prevent the influence of lead wire inductance on the sensitivity.

4. Conclusions

We investigated the displacement dependences on inductance of the coil spring and of output voltage of an AC voltage divider circuit where the coil spring took a part as an inductor for the purpose of a displacement sensor application of a mechanical spring. The changing ratios of inductance and output voltage to displacement were estimated to be 6.6 %/mm and 6.23 %/mm, respectively. As a conclusion, we determined that there is sufficient possibility to apply a mechanical coil spring as a displacement sensor. For practical sensor applications, we found a few problems to be studied at next stage; we should eliminate the influence of lead wire on the sensitivity. This matter is one of important points to design an electronic circuit for the sensor. And we need to analyze quantitatively the change rate of the inductance with respect to the shape and size of coil spring.

Acknowledgement

This research was supported by Kyungsung University Research Grants in 2019.

References

[1] D. Abdul Budan and T. S. Manjunatha, International Journal of Mechanical, Aerospace, Industrial, Mechatronic and Manufacturing Engineering **4**, 1035 (2010).
[2] Eduardo E. Rodríguez and Gabriel A. Gesnouin, The Physics Teacher **45**, 100 (2007).
[3] G. Dehmel, Chapter 6 in Sensors – a comprehensive survey **5**, 205 VCH Publishers (1989) pp 205-254.
[4] P. Ripka, "Induction sensors", Chapter 2 in Magnetic sensors and magnetometers, Artech House (2001) pp 47-74
[5] S. Tumanski, J. Magn. Magn. Mat. **242-245**, 1153 (2002).
[6] R. J. Prance, T. D. Clark, and H. Prance, Rev. Sc. Instr. **74**, 3733 (2003).
[7] K. P. Estola and J. Malmivuo, J. Phys. E **15**, 1110 (1982).
[8] G. Schilstra and J. H. van Hateren, J. Neuroscience Methods **83**, 125 (1998).
[9] R. J. Prance, T. D. Clark, and H. Prance, Sensors and Actuators **85**, 361 (2000).
[10] H. Ueda and T. Watanabe, J. Geomagn. Geoelectr. **32**, 285 (1980).
[11] K. Hayashi, T. Oguti, T. Watanabe, and L. F. Zambresky, J. Geomagn. Geoelectr. **30**, 619 (1978).
[12] N. F. Ness, Space Science Reviews **11**, 459 (1970).
[13] V. E. Korepanow, Adv. Space. Res. **32**, 401 (2003).
[14] V. Korepanov and R. Berkman, Measurement **29**, 137 (2001).
[15] Edward B. Rosa, Bulletin of Bureau of Standards **4**, 301 (1908).
[16] V. T. Morgan, IEEE Trans. Power Deliv. **28**, 1252 (2013).
[17] Xi Nan and C. R. Sullivan, IEEE Power Electronics Specialists Conference, 853 (2003).
[18] H. A. Wheeler, Proc of the IEEE **70**, 1449 (1962).
[19] Richard Ludin, Proc. of the IEEE **73**, 1428 (1985).
[20] H. Nagaoka, J. Coll. Sci. **27**, 18 (1909).
[21] https://www.comsol.com/
[22] R. Lide David. Handbook of Chemistry and of Physics-75h Edition. London: The Chemical Rubber Co. (1995) pp 12-185.
[23] http://sine.ni.com/nips/cds/view/p/lang/ko/nid/201800